Submitted to Physical Review B

LBL-1151

DETERMINATION OF THE SURFACE GEOMETRY FOR THE ALUMINUM (110) AND (111) SURFACES BY COMPARISON OF LEED CALCULATIONS WITH EXPERIMENT

M. R. Martin and G. A. Somorjai

September 1972

AEC Contract No. W-7405-eng-48

For Reference

Not to be taken from this room

LBL-1151

DISCLAIMER

This document was prepared as an account of work sponsored by the United States Government. While this document is believed to contain correct information, neither the United States Government nor any agency thereof, nor the Regents of the University of California, nor any of their employees, makes any warranty, express or implied, or assumes any legal responsibility for the accuracy, completeness, or usefulness of any information, apparatus, product, or process disclosed, or represents that its use would not infringe privately owned rights. Reference herein to any specific commercial product, process, or service by its trade name, trademark, manufacturer, or otherwise, does not necessarily constitute or imply its endorsement, recommendation, or favoring by the United States Government or any agency thereof, or the Regents of the University of California. The views and opinions of authors expressed herein do not necessarily state or reflect those of the United States Government or any agency thereof or the Regents of the University of California.

DETERMINATION OF THE SURFACE GEOMETRY FOR THE ALUMINUM (110) AND (111) SURFACES BY COMPARISON OF LEED CALCULATIONS WITH EXPERIMENT

M. R. Martin and G. A. Somorjai

Inorganic Materials Research Division, Lawrence Berkeley Laboratory
and Department of Chemistry; University of California
Berkeley, California 94720

ABSTRACT

Low energy electron diffraction (LEED) calculations have been extended to the (110) and (111) surfaces of aluminum in order to determine the spacing between the surface and bulk layers of the crystal. The Al (110) surface is found to be contracted by 10% to 15% from the bulk interlayer spacing, and the Al (111) surface is found to deviate from the bulk spacing by less than 5%. This amounts to a determination of the surface layer position to within 0.1Å. Results of calculations on all experimentally measured beams for these surfaces are compared with the experimental results for several assumed interlayer spacings. These comparisons are made with respect to qualitative peak shapes, peak positions and relative peak amplitudes of the specular and all measured non-specular beams from each surface. In order to achieve this agreement, it has been necessary to include the four outermost crystal layers and to describe the ion-core potential with five phase shifts in the 40 eV → 150 eV energy range.

I. INTRODUCTION

In a previous paper[1] (henceforth referred to as MS) we have reported on a series of low energy electron diffraction (LEED) calculations performed on the (100) face of aluminum. In the present work we extend this computational method to the (110) and the (111) surfaces of the same material. The reader is referred to Section I of MS for a description of the computation and for definitions of the quantities to be discussed below. In Fig. 1 we show the LEED beam geometry for typical diffraction patterns from the (110) and (111) surfaces. The beam labels and the azimuthal angle of the incident beam are defined to be identical to those used by Jona.[2] The orientation of the incident beam is described by the azimuthal angle ϕ, and the angle θ, which is measured from a normal to the crystal surface.

One of the results obtained in MS is that theoretical intensity vs incident electron energy (I vs eV) curves of a quality allowing detailed comparison with experimental measurements is possible by including in the calculation only three layers of the crystal parallel to the aluminum (100) surface. This degree of agreement can be achieved in the 40 eV $\rightarrow$ 150 eV energy range by the inclusion of five phase shifts to characertize the ion-core potential within the metal.

In this paper we do not intend to repeat for the (110) and (111) surfaces all the calculations made in MS for the aluminum (100) surface. Many of the points made at that time are equally applicable as exemplified in Fig. 2 where we perform a four layer calculation using 3, 4 and 5 phase shifts. As observed in MS for the aluminum (100) surface, the three phase shift curve is in reasonable qualitative agreement with the other two (using 4 and 5 phase shifts), but yields intensity curves of

about twice the magnitude. The addition of a fourth phase shift reduces the overall magnitude of the curve, and a fifth phase shift introduces significant changes only in the upper portion of the energy range considered. As in the work on the (100) surface of aluminum, we will work mainly with 5 phase shifts when detailed comparison with experimental results is sought.

The use of a limited number of layers parallel to the crystal surface in the computation can be justified by the large inelastic damping factor of electrons in the LEED energy range ($\lesssim$ 200 eV). This damping factor is responsible for attenuating the elastically reflected beams within the crystal. A typical inelastic damping length in aluminum is $\lambda \approx 8$Å,[3] and the interplane separation between planes parallel to the (100) surface is 2.02Å. A singly scattered electron would thus have to travel more than 12Å inside the crystal to be scattered from the fourth layer, and multiply scattered electrons must traverse an even longer path. Justification for using only three layers has been presented in MS for the aluminum (100) surface. The same arguments are applicable to the (111) surface for which the bulk interplane separation of 2.33Å is slightly larger than for the (100) surface.

The interplane spacing between planes parallel to the (110) surface is equal to half the nearest neighbor distance in the crystal, or 1.43Å. Since this is appreciably smaller than the spacing between planes of the (100) and (111) surfaces, it is necessary to determine the minimum number of layers which must be included in a calculation of the (110) surface. In Fig. 3 we plot the results for the (00)-beam of the aluminum (110) face employing 3, 4 and 5 layers parallel to the surface. The

close agreement between the latter two approximations indicates that the inclusion of four layers should suffice for this surface in the energy range of 40 eV → 150 eV.

The results of the calculations to be presented in the following two sections indicate that the position of the surface layer with respect to the bulk can be determined to within ~5% of the bulk interlayer spacing. The Al (110) surface layer is found to be located between 1.285Å and 1.214Å from the next underlying layer which represents a contraction of 10% to 15% of the bulk interlayer spacing. The Al (111) surface layer spacing is found to be equal to the bulk interplane spacing to within ~5%. In each case the surface layer spacing is determined to within 0.1Å.

II. ALUMINUM (110)

Of the three low order surfaces of aluminum, the (110) face has proved to be the most elusive in achieving theoretical agreement with the experimental results. Laramore and Duke[3] have recently investigated the (100), (110) and (111) surfaces using a maximum of three phase shifts and treating the surface region as a simply truncated bulk crystal. They suggest that the discrepancies in the case of the (110) surface could be due to a contraction in the spacing between the two outermost layers of the order of 10%. Houston, Laramore, and Park[4] have taken a different approach and attempt to account for the disagreement between theory and experiment by proposing that the aluminum (110) surface is not a simple planar truncation of the bulk structure, but that stepped regions exist on the surface. In the present work we perform calculations utilizing four and five phase shifts and investigate the effects of displacing the surface layer from the position it would have if the bulk of the crystal were simply terminated.

In Figs. 4 through 7 we present a comparison between the experimental data of Jona[2] for the aluminum (110) surface and calculations we have performed using various models for the surface layer geometry. In these figures we present the results for the (00)-, (10)-, (01)-, and (11)-beams respectively. All curves are computed for a normally incident electron beam except for the dotted curve in Fig. 4(d) for which the beam enters the crystal at an angle $\theta = 5°$ from the surface normal and a azimuthal angle $\phi = 90°$.

In all the computed curves presented in this paper we have used the Lundqvist form for the complex electron self-energy[5]

$\Sigma(E) = \Sigma_1(E) - i\Sigma_2(E)$, and have shifted the final curves by an additional 3.65 eV to account for the work function of the metal.[6] The I vs eV curve 4(a) calculated for the (00)-beam is seen to have its most prominent peak 13 eV lower in energy than the corresponding experimentally observed peak. Similarly the smaller peak near 90 eV is 6 eV lower than experiment. Results obtained for the non-specular beams (Figs. 5 to 7) show the same general characteristic whereby the calculated major and minor peak positions are about 5 eV lower in energy than the experimental values. It has been suggested that a contraction of the spacing between the surface layer and the bulk of the order of 10% might suffice to shift the calculated peak positions into agreement with experiment.[3] In the curves labeled (b), (d) and (e) we perform contractions of 10%, 15% and 20% respectively, yielding surface layer to bulk spacings of 1.285Å, 1.214Å and 1.142Å. The expected energy shift of the peak positions occurs, as well as changes in the ratios of the peak intensities. Comparison of the calculated solid curves of 4(b) and 4(d) with the experimental curve 4(c) shows that the relative intensity ratios of the two prominent (00)-beam peaks is in good agreement with experiment for an outer layer contraction of 10% to 15% of the bulk interlayer spacing. Laramore and Duke[3] have pointed out that the secondary structure obtained in their work near 100 eV in the (00)-beam is too small with respect to their peak near 70 eV. The agreement we have achieved is improved partly due to the contraction we have introduced into the outer layer spacing, and more significantly, as can be seen by reference to Fig. 2, by the inclusion of five phase shifts instead of three. Examination of curve 4(e) indicates that a contraction of 20%, leading to an

outer layer spacing of 1.142Å, shifts the peak appearing near 60 eV to an energy 5 eV in excess of the experimental result. Furthermore, a lower energy peak of about the same magnitude appears to be emerging near 40 eV in contradiction to the observed (00)-beam curve 4(c).

The calculated results for the non-specular beams (Figs. 5 to 7) are likewise seen to improve upon contraction of the outermost layer spacing. The peaks in the 100 eV → 130 eV region for both the (01)- and (10)-beams are seen to shift to higher energies and to diminish in magnitude with respect to the peaks near 50 eV. The results for the (11)-beam are included for completeness, but the absence of multiple prominent peaks makes peak intensity comparisons impossible since only the relative intensities were measured experimentally. The overall qualitative agreement between calculated and experimental non-specular curves appears to occur at an outer layer spacing near 10% and less than 15% contraction from the bulk interlayer distance.

The most serious discrepancies remaining unresolved in the present calculations occur in the 40 eV → 60 eV energy region for the non-specular beams. In Fig. 6 a peak near 50 eV is visible for all the contractions for which we have performed calculations, but the peak never approaches the sharpness of the experimental peak, and this makes it difficult to obtain a meaningful intensity ratio between this peak and the near 105 eV. In Fig. 5 for the (10)-beam, the relative intensities of the two peaks near 45 eV and 65 eV are in good agreement for a layer contraction between 10% and 15%, but the small experimentally observable peak at 56 eV cannot be resolved in these calculations. In Fig. 9 of MS we showed that for the aluminum (100) surface the effect of using an

optical model potential rather than the Lundqvist free electron gas model for the complex self energy gives rise to an energy shift of ~5 eV in the positions of the low energy peaks near 50 eV. The deviations of the calculated peak positions near this energy for layer contractions of 10% to 15% are all within these limits of uncertainty.

In conclusion, we believe that the comparison of all four diffracted beams of Figs. 4 through 7 is sufficient to establish that the spacing between the aluminum (110) surface layer and the bulk is contracted from the bulk interlayer spacing by an amount equal to 10% to 15% of that value, i.e., an interlayer spacing of 1.285Å to 1.214Å. This conclusion is based on the qualitative shapes of all four curves, peak positions and relative peak intensities. We reemphasize the point made in MS that for LEED calculations of presently attainable accuracy it is dangerous to rely exclusively on relative peak amplitudes or on peak positions which may be altered by several eV by small changes in the ion-core potential or by the model used to describe the complex electron self energy $\Sigma(E)$.

III. ALUMINUM (111)

Calculated I vs eV curves are plotted in Figs. 8 through 10 for the (00)-, (10)- and (01)-beams of the aluminum (111) surface. Included in each plot for reference is the experimental curve from the work of Jona[2] (curves (c)). Four calculations are made for each beam. Two of them treat the (111) surface as a simple truncation of the bulk structure and the other two are calculated by assuming a 5% contraction in the spacing between the outermost two layers. The dashed curves in each case represent calculations in which four phase shifts and three layers parallel to the surface are included. The solid curves include five phase shifts and four layers.

For all three beams considered, the calculation using five phase shifts and an undistorted crystal surface yields results in closest agreement with the experimental curves. The calculated peak positions for the (00)-beam are in close agreement with the experimental peaks without making a shift of 4.05 eV to account for the work function of the metal.[6] However, the relative magnitudes of the two peaks are quite different in each case. This is not unexpected since the calculations are performed at normal incidence and the experimental measurements for the (00)-beam are taken at $\phi = 5°$ and $\phi = 30°$. The qualitative agreement between the calculation and experiment is improved by performing the computation for an incident beam impinging at these angles (Fig. 8(d)). The two non-equivalent non-specular beams show similar agreement between the positions of the experimental and theoretical maxima (Figs. 9 and 10). In these cases, moreover, the relative intensities of the various peaks are also in good agreement as are their qualitative shapes.

A rather small outer layer distortion (contraction by 5% of the interlayer spacing, from 2.33Å to 2.216Å) suffices to shift the calculated curves to higher energies, and to qualitatively alter the shapes and intensity ratios of the various peaks. We believe that the cumulative evidence from the three beams considered is sufficient to establish that the spacing between the outermost two layers of the aluminum (111) surface is identical to the bulk spacing to within less than 5%.

The good qualitative agreement attained in this case allows us to point out certain limitations in calculations of this degree of accuracy. The ion-core potential calculated by the method of Pendry[7] is sufficient to give the agreement obtained here, but does not allow the resolution of the 50 eV → 60 eV peak of the (01)-beam into the double peak structure seen in the experimental curve. A similar instance was noted in the previous section for the (10)-beam of the aluminum (110) surface in the same energy region. Discrepancies in the low energy ($\lesssim$ 50 eV) peak positions for the (111) surface are of the same magnitude as those observed with the (110) surface and indicate that such effects are attributable to the form of the ion-core potential, or to the model employed for the complex electron self energy rather than to the geometrical arrangement of the crystal layers in the surface region.

ACKNOWLEDGEMENTS

This work was supported by the U. S. Atomic Energy Commission. We are grateful to Dr. J. B. Pendry for supplying the computer program used to calculate the ion-core phase shifts.

0 0 0 0 3 8 0 0 7 9 7

REFERENCES

1. M. R. Martin and G. A. Somorjai, Phys. Rev.
2. F. Jona, IBM Journal of Res. and Dev. 14 (4), (July 1970).
3. G. E. Laramore and C. B. Duke, Phys. Rev. B5, 267 (1972).
4. Houston, Laramore and Park, Surface Science (to be published).
5. B. I. Lundqvist, Phys. Stat. Sol. 32, 273 (1969).
6. N. D. Lang and W. Kohn, Phys. Rev. B3, 1215 (1971).
7. J. B. Pendry, J. Phys. (Sol. State Physics) 4, 2501 (1971).

FIGURE CAPTIONS

Fig. 1. Low energy electron diffraction spot positions for (a) the (110) surface and (b) the (111) surface of aluminum. The spot labels and the azimuthal angles ϕ are defined to be identical to those of Jona.[2]

Fig. 2. Comparison of I vs eV curves computed using 3, 4 and 5 phase shifts for the aluminum (110) surface.

Fig. 3. Comparison of I vs eV curves computed using 4 phase shifts and 3, 4 and 5 crystal layers parallel to the aluminum (110) surface.

Fig. 4. The experimental I vs eV curve (c) is compared to calculated curves for the (00)-beam of the aluminum (110) surface. The solid curves (a, b, d) and the dotted curve (d) utilize 5 phase shifts and 4 layers in the computation. The dashed curves utilize 4 phase shifts and 4 layers. Curve (a) is obtained from an undistorted surface (i.e., interlayer spacing equal to the bulk value 1.43Å). In curve (b) the outer layer spacing is contracted by 10% to 1.285 Å. In curve (d) the outer layer is contracted by 15% to 1.214 Å, and in curve (e) it is contracted by 20% from the bulk value to 1.142 Å. The theoretical curves are all shifted by 3.65 eV to account for the metallic work function.

Fig. 5. The experimental I vs eV curve (c) is compared to calculated curves for the (10)-beam of the aluminum (110) surface. The descriptions of curves a → e are given in the caption to Fig. 4.

Fig. 6. The experimental I vs eV curve (c) is compared to calculated curves for the (01)-beam of the aluminum (110) surface. The descriptions of curves a → e are given in the caption to Fig. 4.

Fig. 7. The experimental I vs eV curve (c) is compared to calculated curves for the (11)-beam of the aluminum (110) surface. The descriptions of curves a → e are given in the caption to Fig. 4.

Fig. 8. The experimental I vs eV curve (c) is compared to calculated curves for the (00)-beam of the aluminum (111) surface. The solid curves (a, b and d) utilize 5 phase shifts and 4 layers in the computation. The dashed curves (a) and (b) utilize 4 phase shifts and 3 layers. Curve (a) is obtained from a surface whose outer layer spacing is contracted by 5% of the bulk value to 2.216 Å. Curve (b) is obtained from an undistorted surface in which the outer layer spacing is equal to that in the bulk, 2.33 Å. Curve (d) is computed for an electron beam incident at $\theta = 5°$ and $\phi = 30°$ with a surface layer spacing equal to that in the bulk. The theoretical curves are all shifted by 4.05 eV to account for the metallic work function.

Fig. 9. The experimental I vs eV curve (c) is compared to calculated curves for the (10)-beam ($= \bar{1}1 = 0\bar{1}$) of the aluminum (111) surface. The description of curves (a) and (b) are given in the caption to Fig. 8.

Fig. 10. The experimental I vs eV curve (c) is compared to calculated curves for the (01)-beam ($= \bar{1}0 = 1\bar{1}$) of the aluminum (111) surface. The description of curves (a) and (b) are given in the caption to Fig. 8.

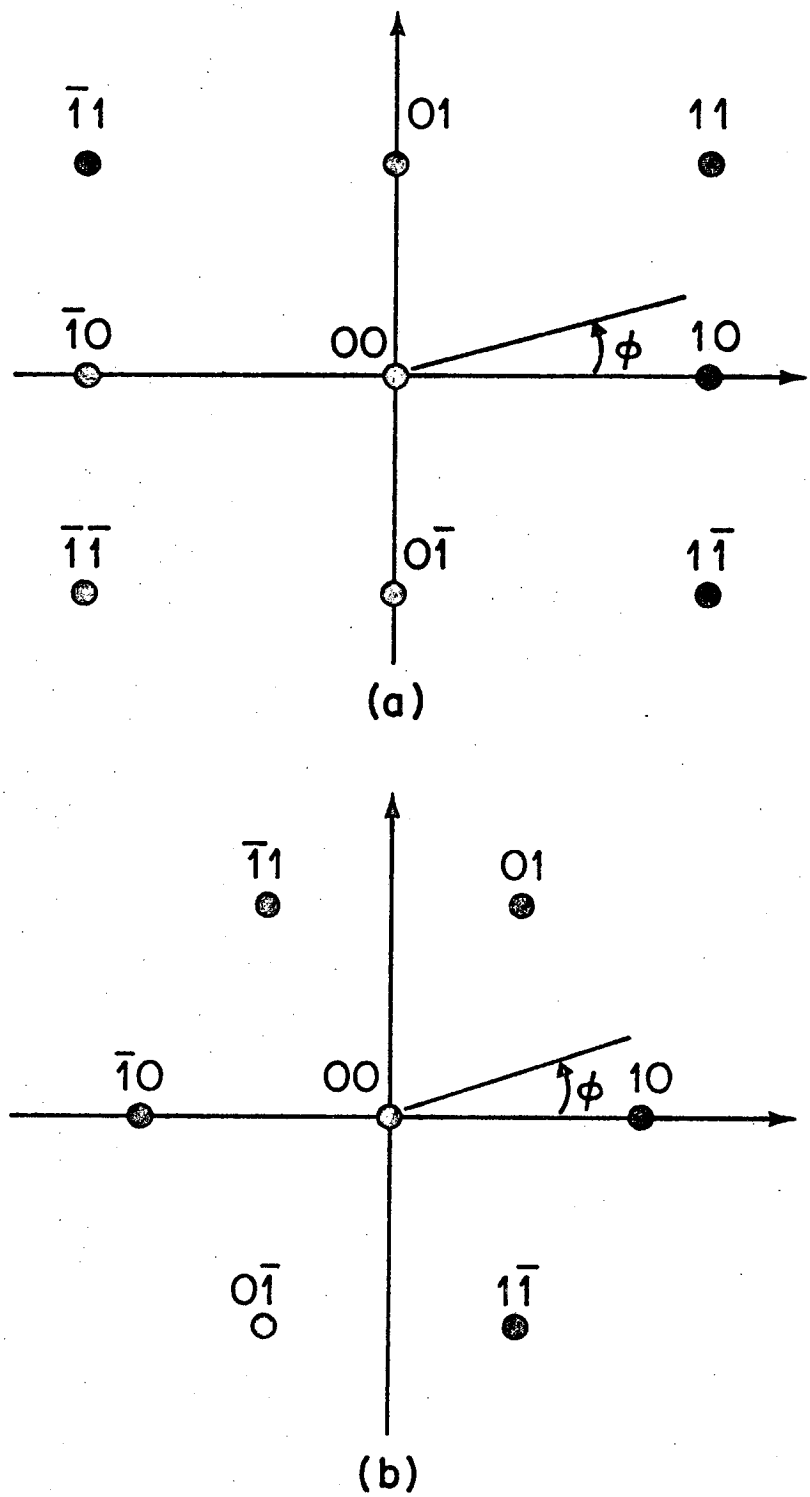

XBL728-6877

Fig. 1

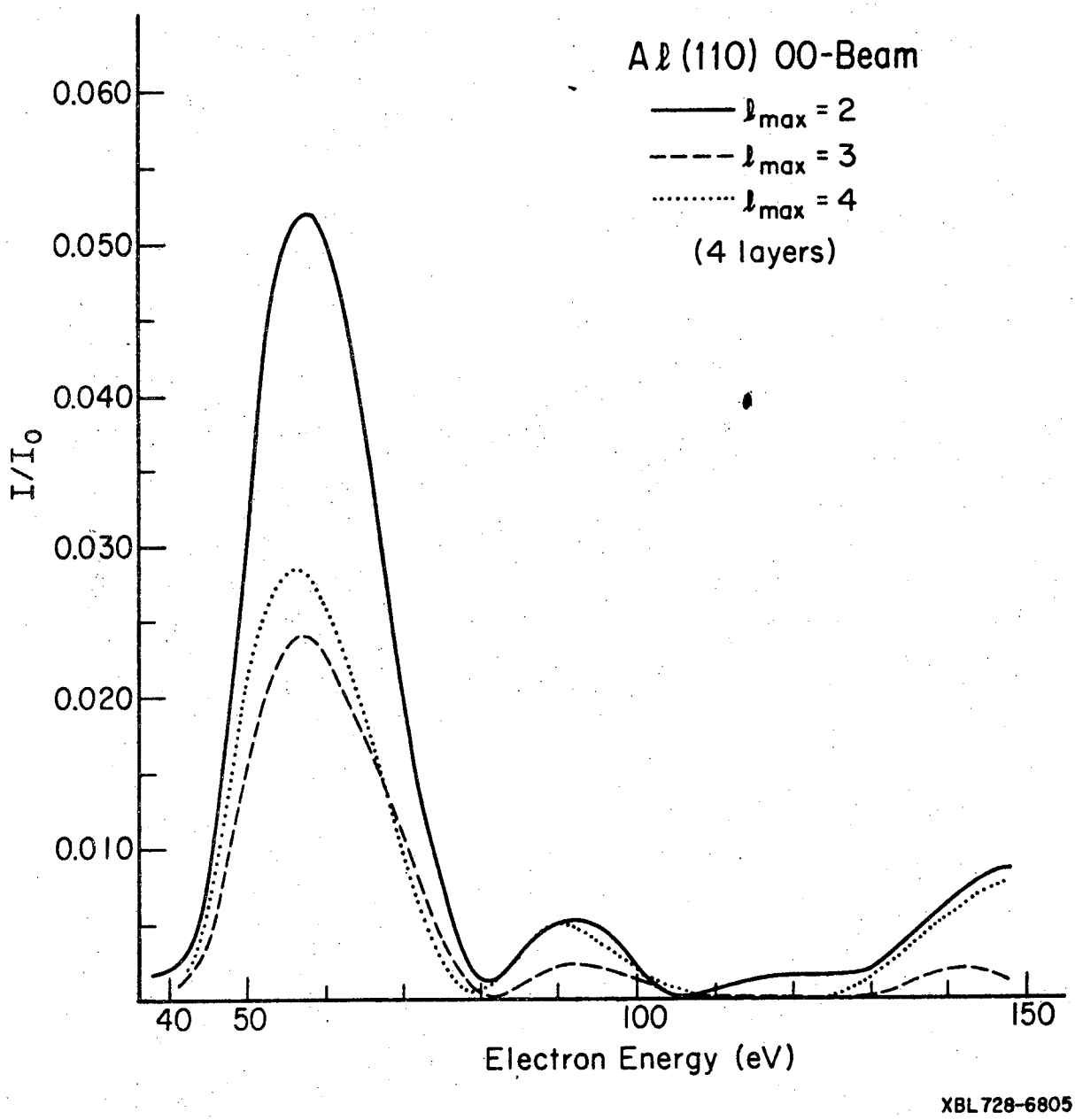
Aℓ (110) 00-Beam
ℓmax = 2
ℓmax = 3
ℓmax = 4
(4 layers)
0.060
0.050
0.040
0.030
0.020
0.010
I/I0
40
50
100
150
Electron Energy (eV)
XBL728-6805

Fig. 2

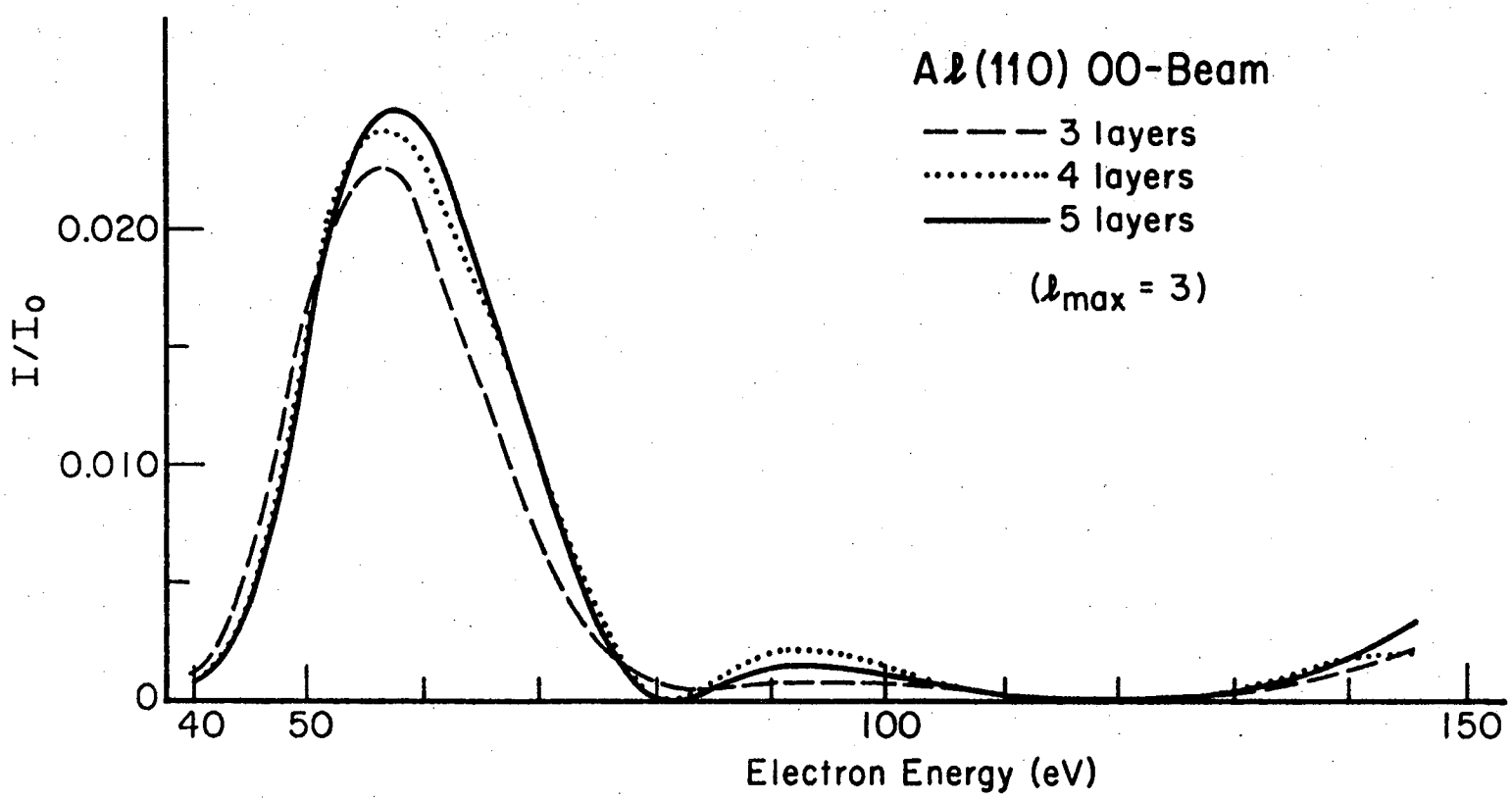

XBL728-6800

Fig. 3

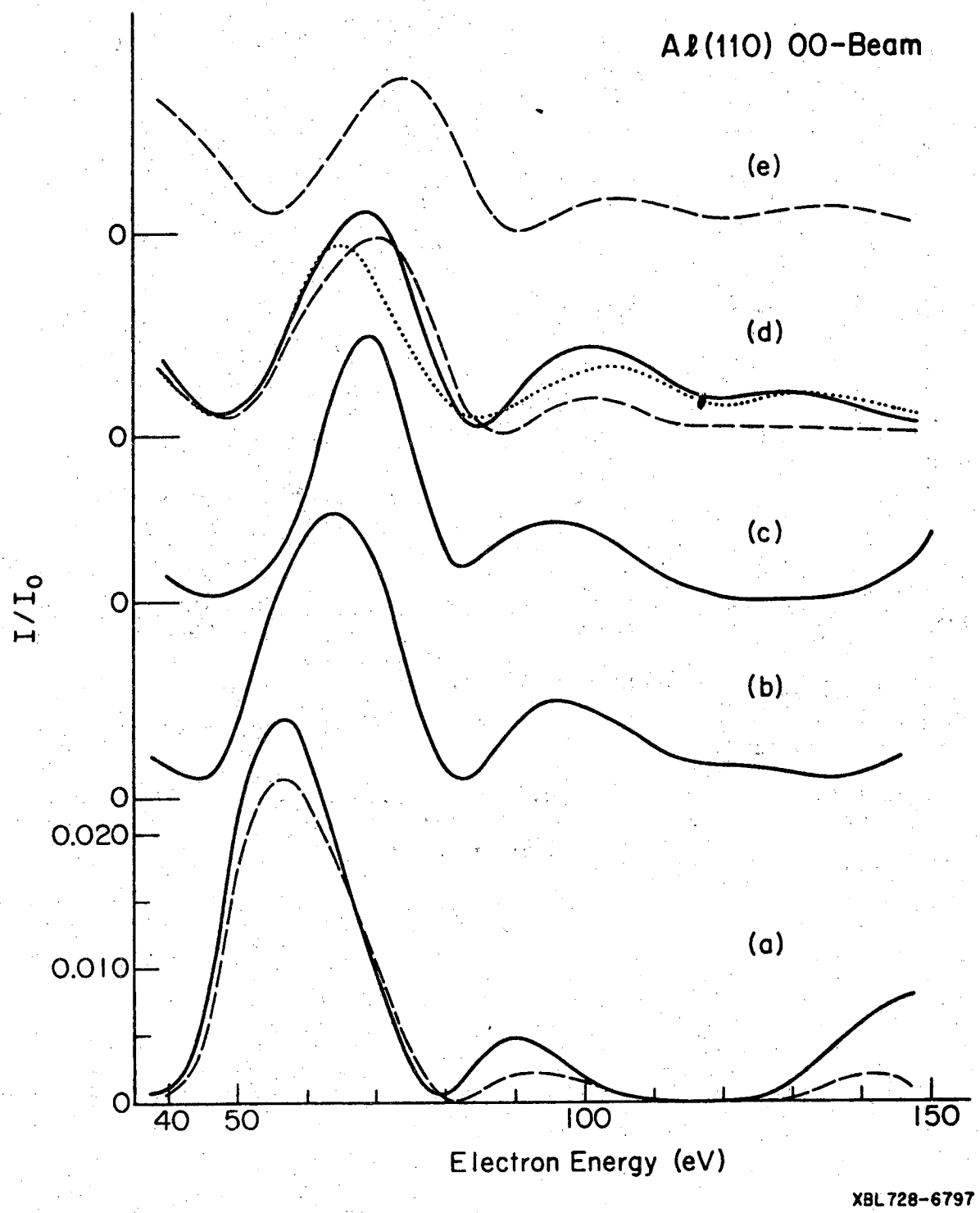
Aℓ(110) 00-Beam
(e)
(d)
(c)
(b)
(a)
I/I₀
0
0
0
0
0
0.020
0.010
0
40
50
100
150
Electron Energy (eV)
XBL 728-6797

Fig. 4

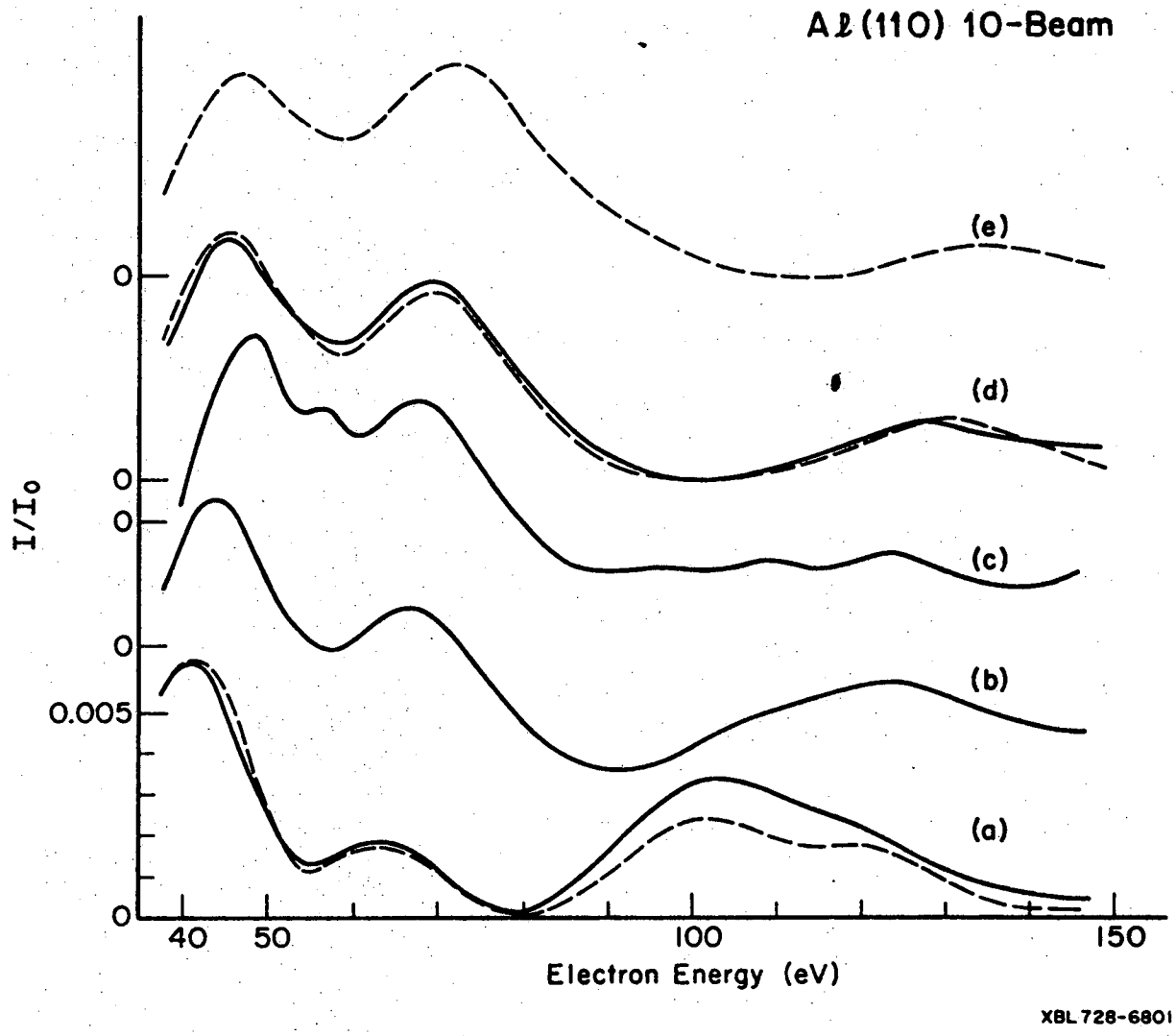
Aℓ(110) 10-Beam
(e)
(d)
(c)
(b)
(a)
I/I₀
0
0
0
0
0.005
0
40
50
100
150
Electron Energy (eV)
XBL 728-6801

Fig. 5

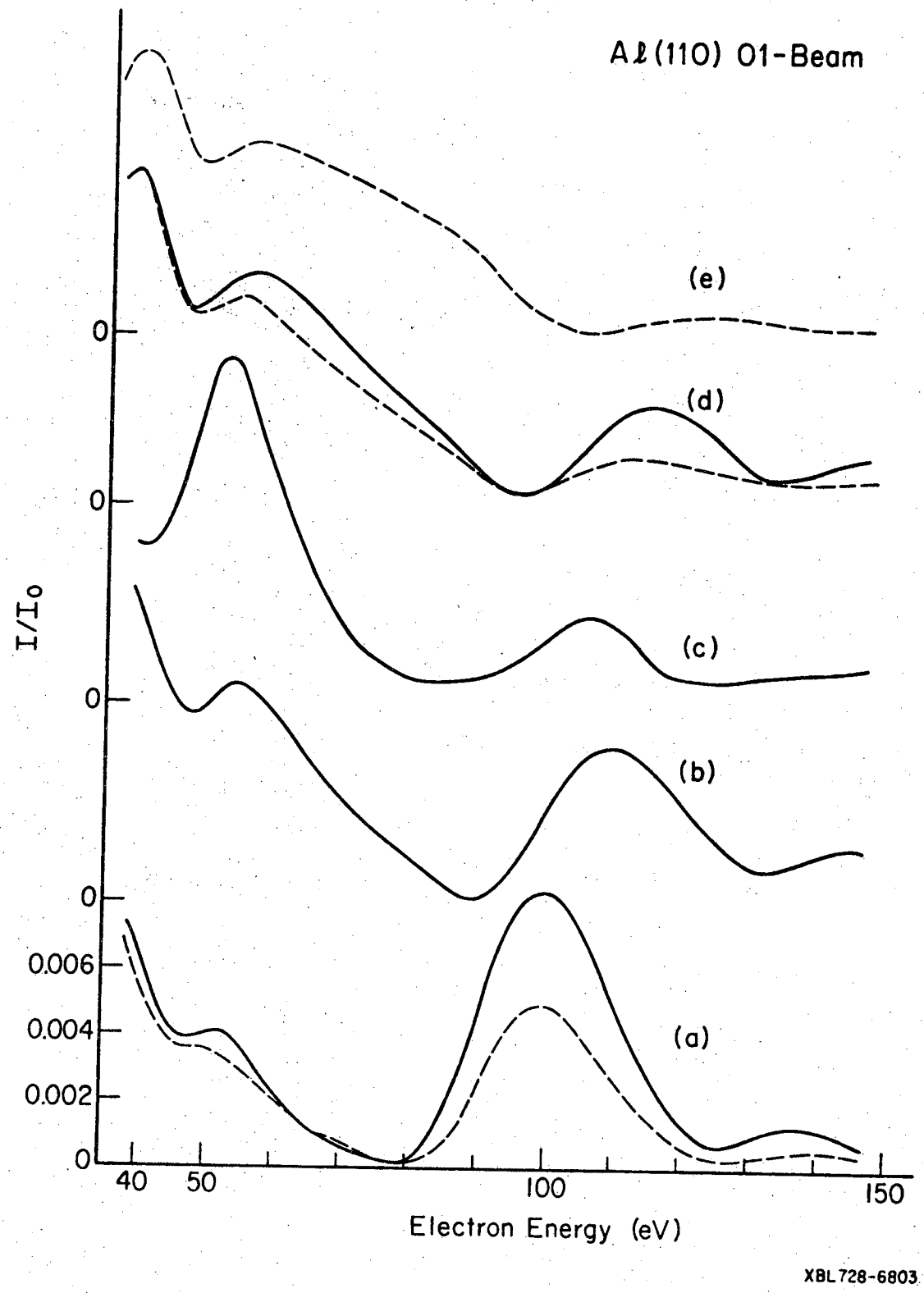
Aℓ(110) 01-Beam
(e)
(d)
(c)
(b)
(a)
I/I₀
0
0
0
0
0.006
0.004
0.002
0
40
50
100
150
Electron Energy (eV)
XBL728-6803

Fig. 6

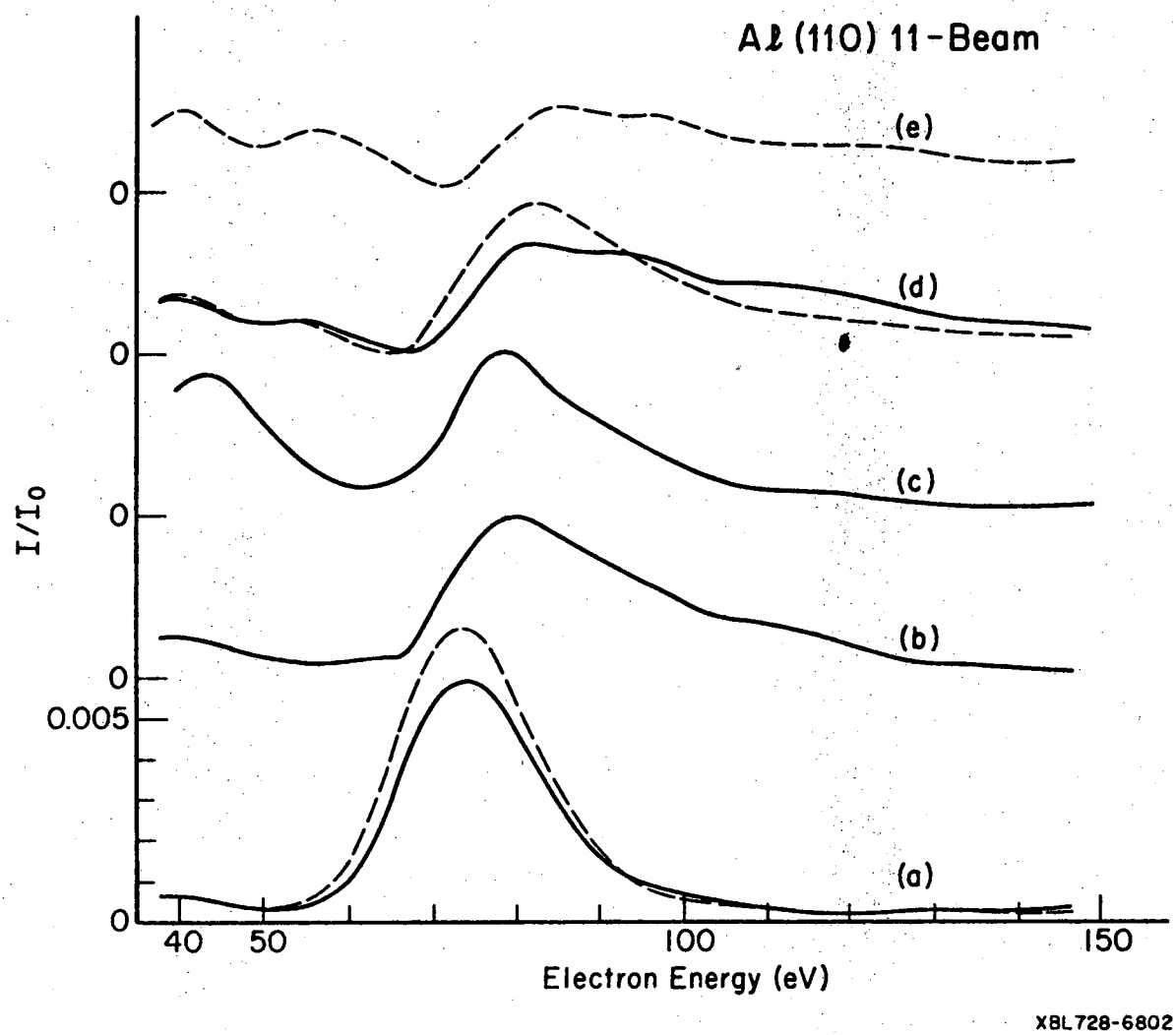
Aℓ (110) 11-Beam
(e)
(d)
(c)
(b)
(a)
I/I₀
0
0
0
0
0.005
0
40
50
100
150
Electron Energy (eV)
X8L728-6802

Fig. 7

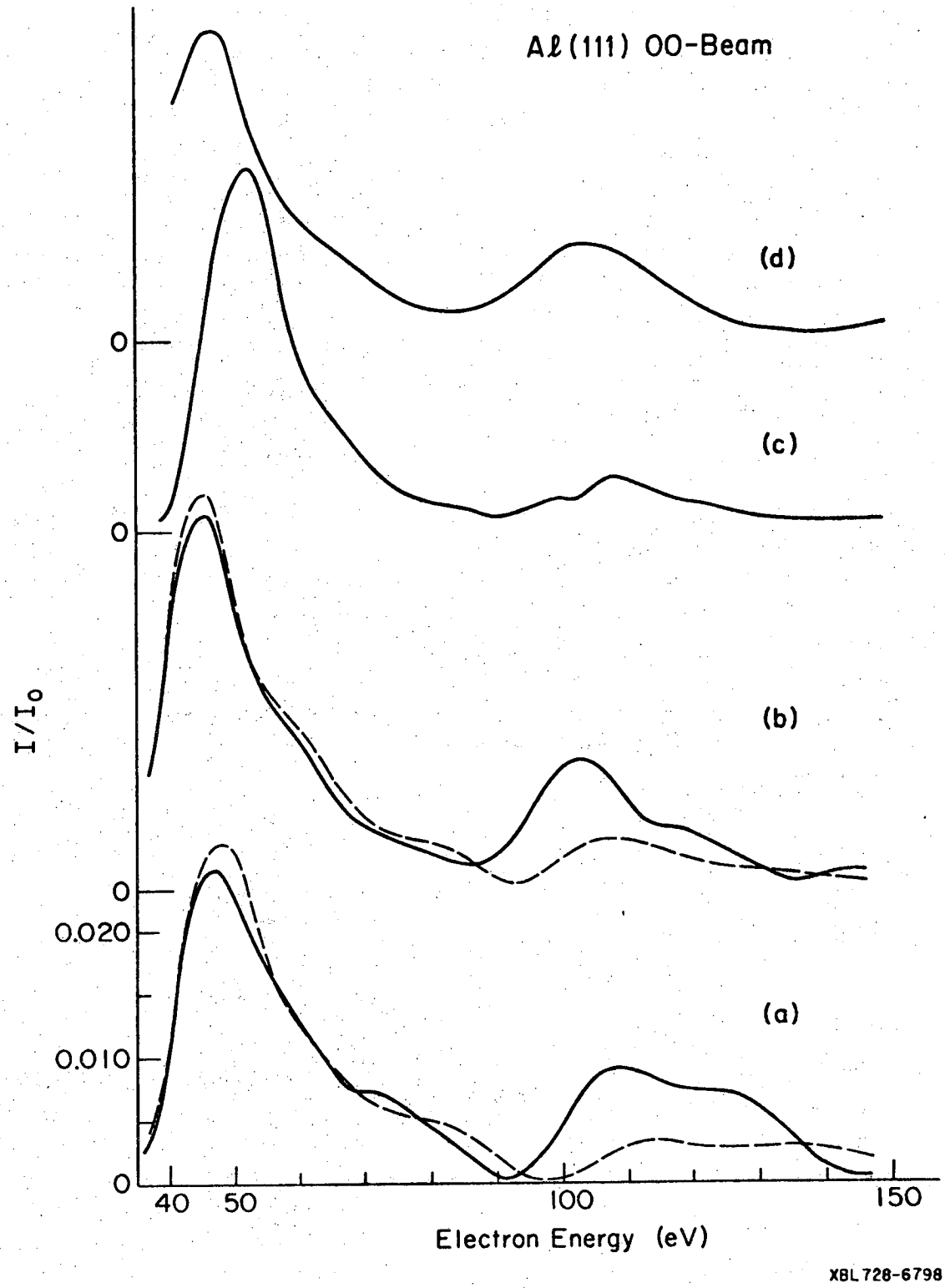
Aℓ(111) 00-Beam
(d)
(c)
(b)
(a)
0
0
0
0
0.020
0.010
I/I₀
40
50
100
150
Electron Energy (eV)
XBL 728-6798

Fig. 8

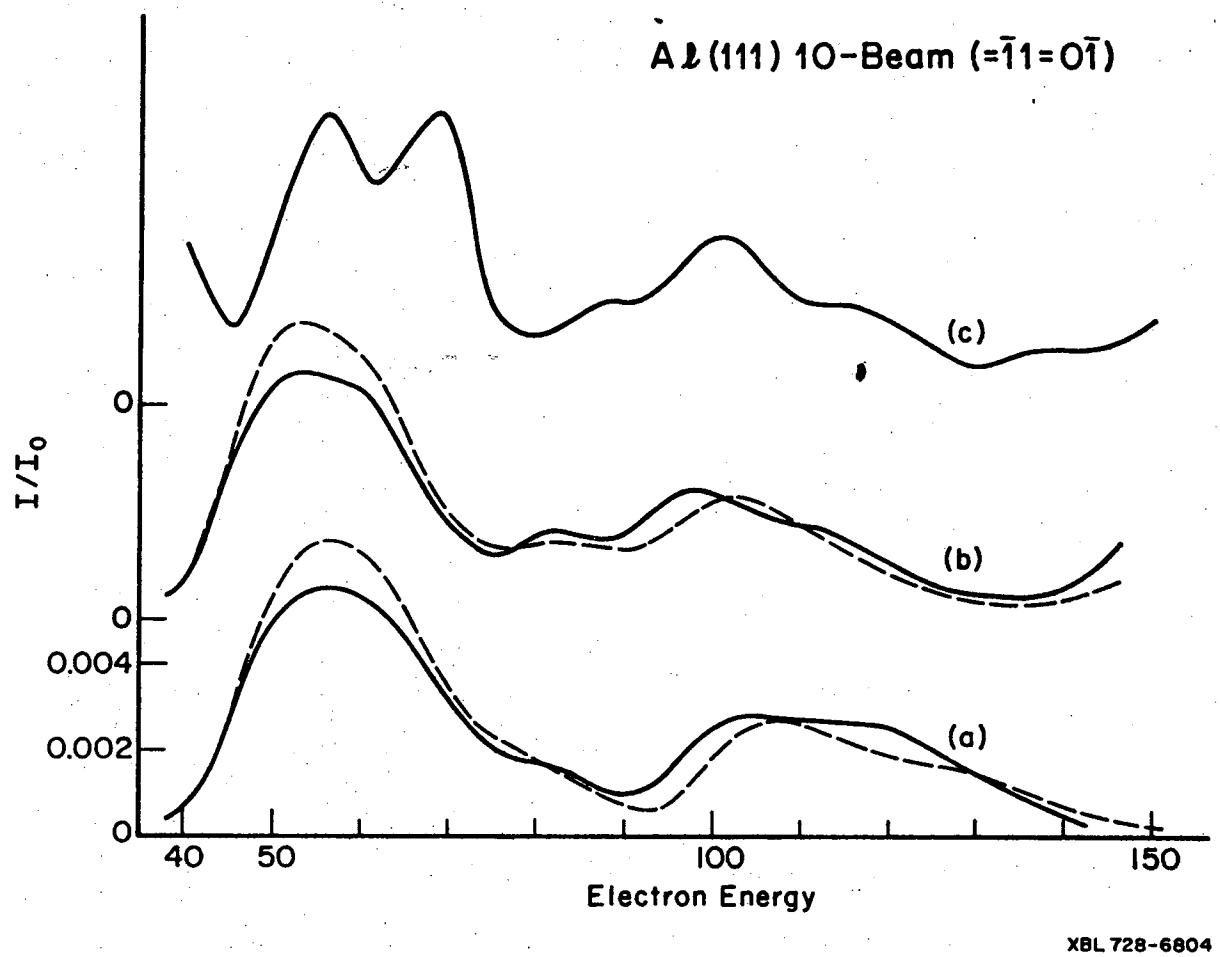
Aℓ(111) 10-Beam (=$\bar{1}$1=0$\bar{1}$)
(c)
(b)
(a)
I/I$_0$
0
0
0.004
0.002
0
40
50
100
150
Electron Energy
XBL 728-6804

Fig. 9

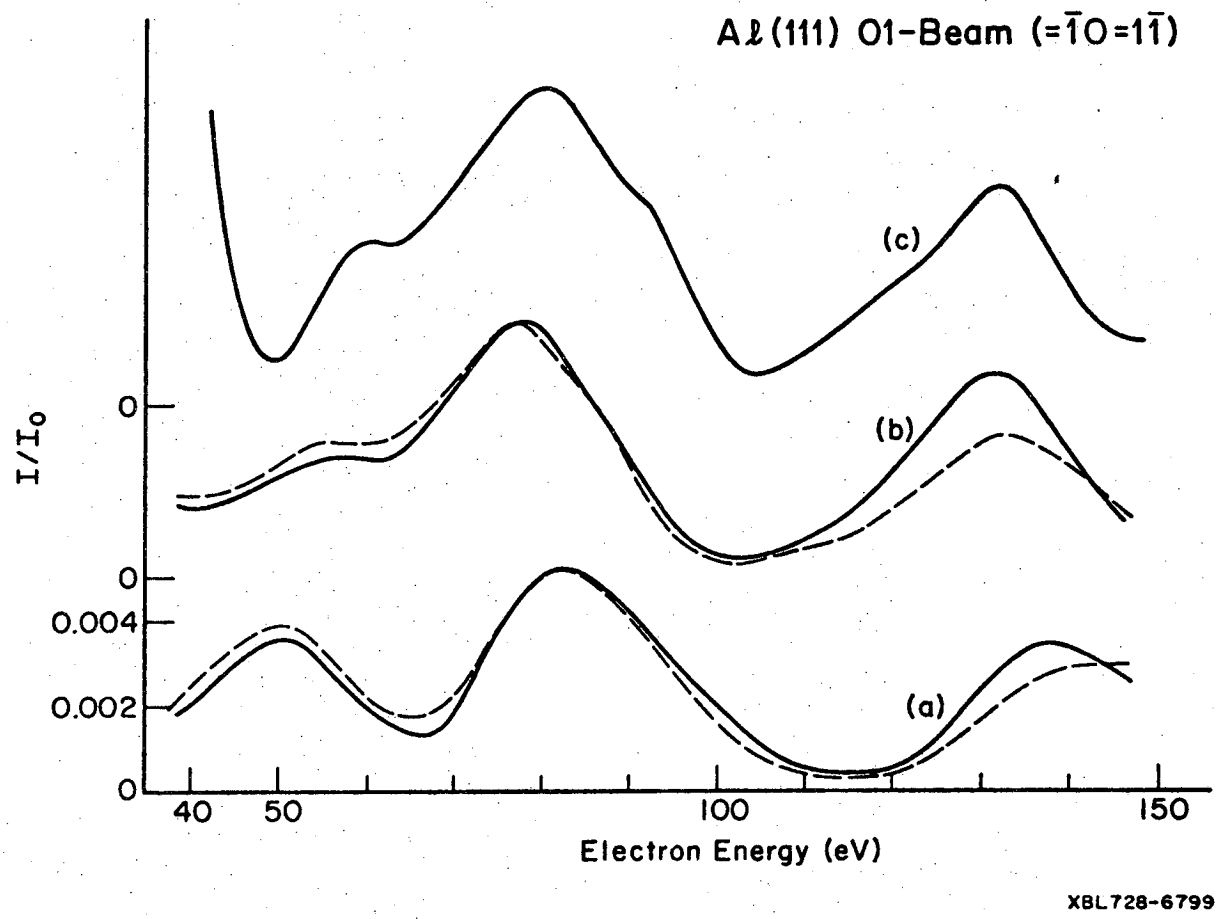
Aℓ(111) 01-Beam (=$\bar{1}$0=1$\bar{1}$)
(c)
(b)
(a)
I/I$_0$
0
0
0.004
0.002
0
40
50
100
150
Electron Energy (eV)
XBL728-6799

Fig. 10

LEGAL NOTICE

This report was prepared as an account of work sponsored by the United States Government. Neither the United States nor the United States Atomic Energy Commission, nor any of their employees, nor any of their contractors, subcontractors, or their employees, makes any warranty, express or implied, or assumes any legal liability or responsibility for the accuracy, completeness or usefulness of any information, apparatus, product or process disclosed, or represents that its use would not infringe privately owned rights.

TECHNICAL INFORMATION DIVISION
LAWRENCE BERKELEY LABORATORY
UNIVERSITY OF CALIFORNIA
BERKELEY, CALIFORNIA 94720